Cell Systems

Math | Bio

# Self-Amplifying Pulsatile Protein Dynamics without Positive Feedback

## Graphical Abstract

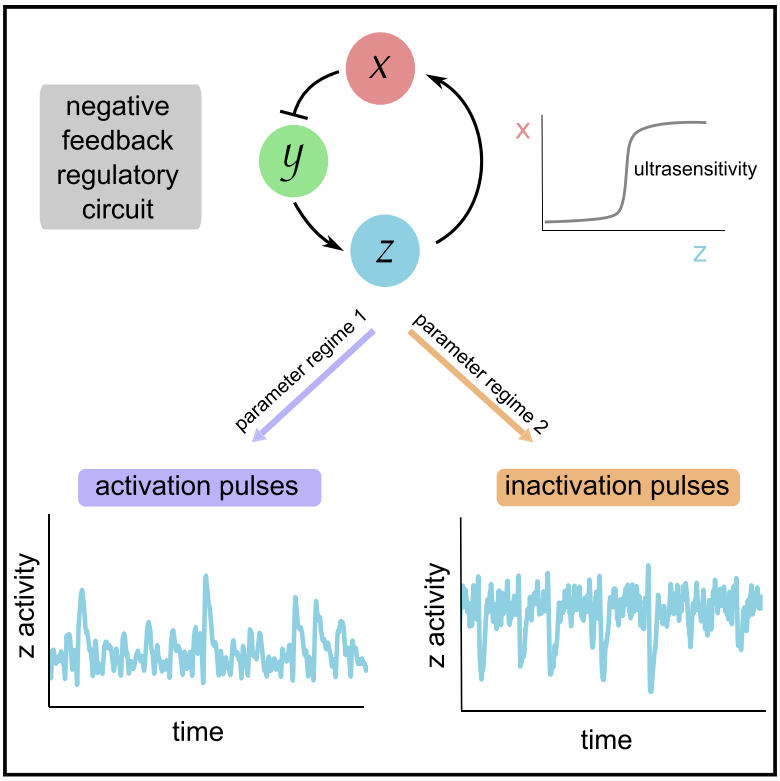


## Authors

Rosa Martinez-Corral, Elba Raimundez, Yihan Lin, Michael B. Elowitz, Jordi Garcia-Ojalvo

## Correspondence

jordi.g.ojalvo@upf.edu

## In Brief

Stochastic pulses in protein activity can be generated from a regulatory circuit with only a negative feedback, provided one of the interactions in the feedback loop is ultrasensitive. Positive feedback, which is usually thought to be required for these dynamics, is dispensable. The same circuit architecture can support both activation and inactivation pulses depending on the parameter regime.

## Highlights

- Stochastic pulses can arise from a protein circuit with only a negative feedback
- Pulsing requires ultrasensitivity and adequate separation of timescales
- Both activation and inactivation pulses of a target protein can be generated

Martinez-Corral et al., 2018, Cell Systems 7, 453–462
October 24, 2018 © 2018 Elsevier Inc.
https://doi.org/10.1016/j.cels.2018.08.012

CellPress

Cell Systems
Math | Bio

CellPress

# Self-Amplifying Pulsatile Protein Dynamics without Positive Feedback

Rosa Martinez-Corral,[1] Elba Raimundez,[2,3] Yihan Lin,[4,5] Michael B. Elowitz,[6] and Jordi Garcia-Ojalvo[1,7,*]
[1]Department of Experimental and Health Sciences, Universitat Pompeu Fabra, Barcelona Biomedical Research Park (PRBB), Dr. Aiguader 88, Barcelona 08003, Spain
[2]Helmholtz Zentrum München-German Research Center for Environmental Health, Institute of Computational Biology, Neuherberg 85764, Germany
[3]Center for Mathematics, Chair of Mathematical Modeling of Biological Systems, Technische Universität München, Garching 85748, Germany
[4]Center for Quantitative Biology and Peking-Tsinghua Joint Center for Life Sciences, Academy for Advanced Interdisciplinary Studies, Peking University, Beijing 100871, China
[5]The MOE Key Laboratory of Cell Proliferation and Differentiation, School of Life Sciences, Peking University, Beijing 100871, China
[6]Howard Hughes Medical Institute, Division of Biology and Biological Engineering, California Institute of Technology, Pasadena, CA 91125, USA
[7]Lead Contact
*Correspondence: jordi.g.ojalvo@upf.edu
https://doi.org/10.1016/j.cels.2018.08.012

## SUMMARY

**Many proteins exhibit dynamic activation patterns in the form of irregular pulses. Such behavior is typically attributed to a combination of positive and negative feedback loops in the underlying regulatory network. However, the presence of positive feedbacks is difficult to demonstrate unequivocally, raising the question of whether stochastic pulses can arise from negative feedback only. Here, we use the protein kinase A (PKA) system, a key regulator of the yeast pulsatile transcription factor Msn2, as a case example to show that irregular pulses of protein activity can arise from a negative feedback loop alone. Simplification to two variables reveals that a combination of zero-order ultrasensitivity, timescale separation between the activator and the repressor, and an effective delay in the feedback are sufficient to amplify a perturbation into a pulse. The same circuit topology can account for both activation and inactivation pulses, pointing toward a general mechanism of stochastic pulse generation.**

## INTRODUCTION

Tight regulation of cellular processes is essential in all living systems. Generally, this is achieved by networks of interacting biochemical species that sense and transduce input signals and orchestrate a proper response to the environment. Besides simply turning on or off the activity or the levels of cellular components, cells also use dynamics in the form of pulses to encode and convey information. In this case, not only the amplitude but also the duration and number or frequency of pulses can be informative of signal strength and identity (Levine et al., 2013; Martinez-Corral and Garcia-Ojalvo, 2017; Purvis and Lahav, 2013).

Pulses can have a characteristic period, leading to approximately regular oscillations. This is the case of the circadian clock (Goldbeter and Berridge, 1996) and of multiple mammalian proteins such as the tumor suppressor p53 (Geva-Zatorsky et al., 2006), the transcription factor NF-kappaB (Zambrano et al., 2016), and the protein kinases p38 (Tomida et al., 2015) and ERK (Shankaran et al., 2009), among others. To generate periodic oscillations, the system must have a negative feedback interaction between its components (Novák and Tyson, 2008), which can also be accompanied by a positive feedback that helps tune oscillatory behavior (Guantes and Poyatos, 2006; Tsai et al., 2008).

In contrast to periodic pulses, stochastic pulsatile activity without a predominant period is also relevant in cells. This has been reported, for instance, also in ERK (Albeck et al., 2013; Aoki et al., 2013) and p53 (Loewer et al., 2010), in a number of yeast transcription factors including Crz1 (Cai et al., 2008), Msn2 (Garmendia-Torres et al., 2007; Gonze et al., 2008; Hao and O'Shea, 2011; Jacquet et al., 2003), Mig1 (Dalal et al., 2014; Lin et al., 2015), and even in bacteria, with examples such as the entry into the competent state in *Bacillus subtilis* (Schultz et al., 2007; Süel et al., 2006) and the general stress-response factor $\sigma^B$ (Locke et al., 2011). In these cases, the mechanisms underlying pulse generation are diverse and not always well understood.

Currently known mechanisms for stochastic pulse generation can be broadly classified into two groups. One group is mechanisms where the system is readily activated to its maximal level and switched off later on by an inhibitor. This has been proposed to occur in genes regulated by negative feedback, as a result of random switching from the inactive to the active promoter state and the subsequent inhibitor production that eventually switches gene expression off (Zambrano et al., 2015; Zavala and Marquez-Lago, 2014). In this case, there is no amplification of the initial perturbation. Similarly, an incoherent feed-forward architecture, where the input simultaneously activates the target and a repressor of the target (Mangan et al., 2006), can also produce pulsatile behavior without amplifying any initial fluctuation. In contrast, the majority of experimentally reported stochastic pulsatile systems rely on the amplification of an initial

**Box 1. A Motivational Case Study: Stochastic Pulsing in Yeast PKA**

Msn2 is a yeast transcription factor that translocates between the nucleus and the cytoplasm in a pulsatile manner (Görner et al., 1998; Jacquet et al., 2003). Different stresses can differentially modulate pulse amplitude, duration, and frequency, with pulses being particularly relevant under glucose deprivation conditions (Hao and O'Shea, 2011). Msn2 contains nuclear localization and export sequences that are controlled by phosphorylation, which favors nuclear exit (Görner et al., 1998). Although multiple kinases and phosphatases have been shown to be involved in Msn2 localization (Petrenko et al., 2013), there is strong evidence for PKA being a key regulator (Garmendia-Torres et al., 2007; Görner et al., 1998, 2002; Hao et al., 2013; Hao and O'Shea, 2011; Jacquet et al., 2003; Sunnåker et al., 2013). PKA is well known to be regulated by negative feedback, and seminal work established Msn2 pulses as limit cycle oscillations due to negative feedback in the PKA system (Garmendia-Torres et al., 2007; Gonze et al., 2008). However, Msn2 pulses are highly irregular (Box Figure A; Hao and O'Shea, 2011; Lin et al., 2015). Most pulse durations are around 2 min (Box Figure B), but the distribution of interpulse intervals lacks a clear mode, spanning over almost two orders of magnitude, from a few minutes to hours (Box Figure C). The amplitude distribution is also wide (Box Figure D). These observations are more consistent with stochastic pulses rather than with noisy periodic oscillations. Although there are reports hinting at a positive feedback in the PKA system through the kinase Snf1 (Barrett et al., 2012; Jiang et al., 2017; Nicastro et al., 2015), this interaction is very difficult to demonstrate *in vivo* directly and unequivocally. This leaves the door open to the idea that other mechanisms could, in principle, explain the same observations. We hypothesized that the negative feedback regulation of PKA could be sufficient to generate stochastic pulses. Our aim here is not to describe the full behavior of Msn2, which clearly depends on multiple cellular elements but rather to take it as a motivation to study the generation of stochastic pulses from negative feedback.

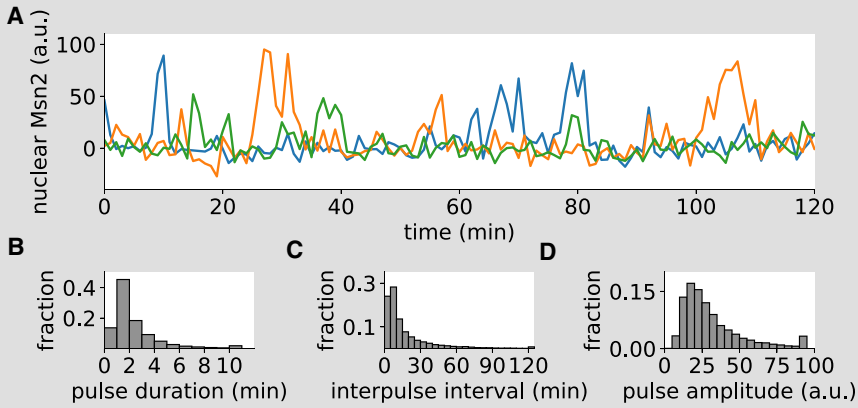


**Box Figure. Stochastic Pulses of Msn2 Nuclear Localization**

(A) Representative time traces of three cells under constant media conditions (0.075% glucose).

(B) Distribution of pulse durations.

(C) Distribution of interpulse intervals (time between consecutive peaks).

(D) Distribution of pulse amplitudes. Histograms are from a time series of cells in the same condition as in (A) and normalized by the total number of data points. Data are the same as in Lin et al. (2015).

perturbation by positive feedback and its subsequent return to basal level by negative feedback. This mechanism has been proposed to act in the *Bacillus subtilis* sin operon, where SinR represses its own transcription and that of SinI while the two proteins cross-inhibit their activity (thus forming a mixed positive and negative feedback) (Voigt et al., 2005). The same mechanism based on a protein-antagonist operon arrangement has been shown to underlie pulses in $\sigma^B$ (Locke et al., 2011). In this case, the process involves zero-order ultrasensitivity, a well-studied phenomenon whereby small changes in the activity of a saturated enzyme lead to much larger relative changes in its target (Goldbeter and Koshland, 1981). In other cases, systems have been described to operate in excitable regimes, where the combination of positive and negative feedback interactions are such that a small fluctuation forces the system to undergo a stereotypic, large excursion in phase space that results in a pulse (Rué and Garcia-Ojalvo, 2011; Süel et al., 2006). In all these, a positive feedback is required for pulsing, which raises the question of whether stochastic pulses arise in systems without this type of interaction, where any other mechanisms to amplify fluctuations might be at play.

Here, we aimed to explore the capacity of negative feedback to generate noise-driven stochastic pulses on its own, taking the PKA pathway (Box 1) as an idealized model. Starting with a minimal model of the PKA protein circuit and further simplifying it into architectures of decreasing dimensionality, we show that a negative feedback with components working in the zero-order kinetics regime, together with correct timescales, is able to respond to a small fluctuation in the levels of one component with a comparatively large pulse. This mechanism can generate both activation and inactivation pulses, showing how negative feedbacks could underlie stochastic pulses driven by noise in a variety of systems.

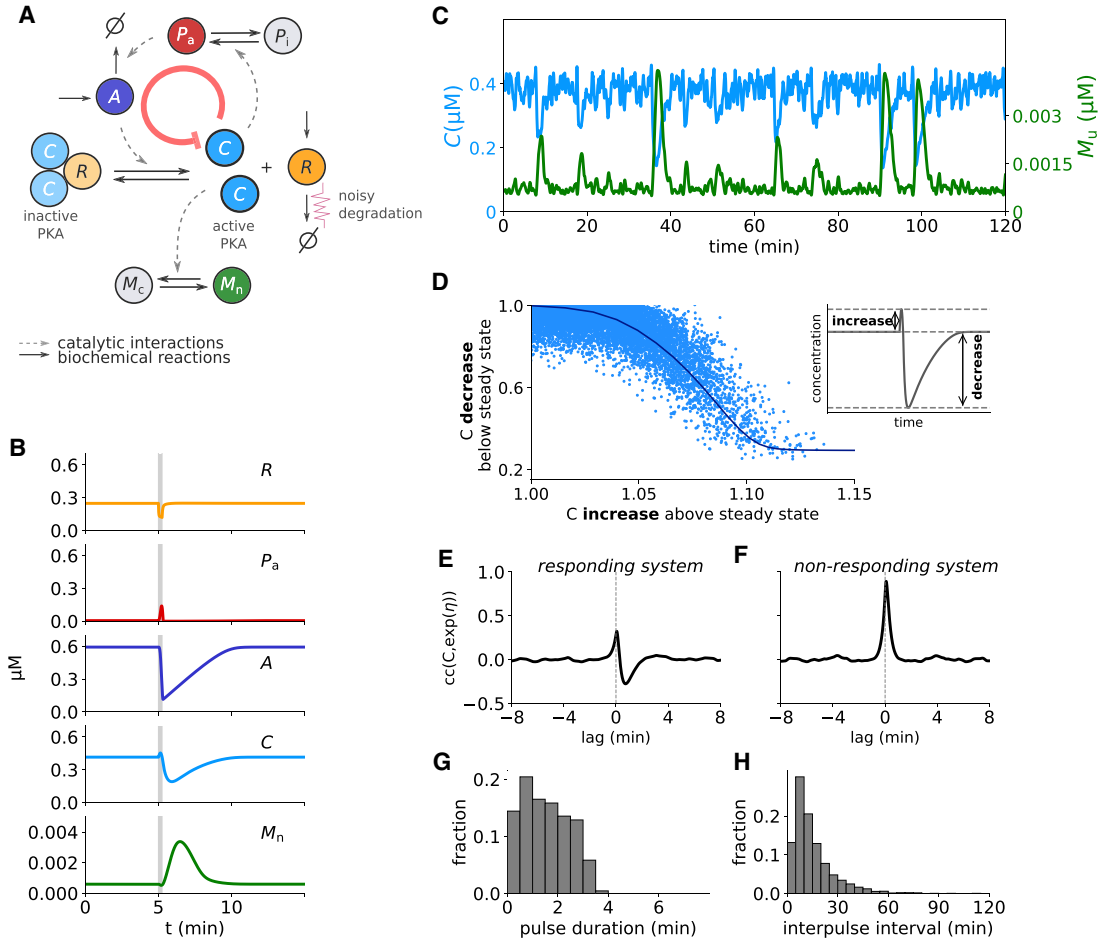


**Figure 1. Stochastic Pulses Can Arise from a Negative Feedback in the PKA Pathway**

(A) Model of the PKA pathway (see text preceding and following Equations 1-4 for details).

(B) In response to an increase in the $R$ degradation rate $\delta$ by a factor 2 during 15 s (gray shaded area), the system exhibits a pulse of $C$ inactivation. Model parameters: $\alpha$ = 23 $\mu M^{-2}min^{-1}$, $\beta$ = 17.4 $\mu M^{-2}min^{-1}$, $\Lambda$ = 6.5 $\mu Mmin^{-1}$, $\delta$ = 26.2 $min^{-1}$, $k_s$ = 0.12 $\mu Mmin^{-1}$, $k_d$ = 25.5 $min^{-1}$, $k_3$ = 0.05 $\mu M$, $\gamma$ = 46.4 $min^{-1}$, $\varepsilon$ = 20 $\mu Mmin^{-1}$, $P_{tot}$ = 0.2 $\mu M$, $k_1$ = 0.0003 $\mu M$, $k_2$ = 0.0002 $\mu M$, $a$ = 0.015 $\mu Mmin^{-1}$, $b$ = 0.06 $min^{-1}$, $k_4$ = 0.0005 $\mu M$, $k_5$ = 0.0005 $\mu M$, and $M_{tot}$ = 0.0052 $\mu M$.

(C) The system exhibits downregulation pulses in $C$ which drive $M_n$ pulses under noisy $\delta$. Stochastic simulations of the same parameter regime as in (B), with $\tau$ = 15 s, $D$ = 0.07, and a time step of $10^{-5}$ min.

(D) The input-output response of the system, normalized with respect to the steady-state value. The solid line is computed from the deterministic model as in (B), for different factors of increases in $\delta$. The dots are the results from a stochastic simulation over 200 hr of simulated time, computed from consecutive relative maxima and minima. Inset schematizes what we consider an increase and decrease, which is normalized by the steady-state level.

(E) Cross-correlation between exp($\eta$) and $C$ for the same simulation conditions as in (C).

(F) Cross-correlation between exp($\eta$) and $C$ for a simulation with the same parameters as in (C) for Equations 1, 6, and 7 but the other rates set to 0.

(G and H) Distribution of $M_n$ pulse duration and interpulse intervals, based on a threshold in $M_n$ of 0.0015 $\mu M$. Data are from 3 simulations of 200 hr with the same parameters as in (C). Interpulse intervals are taken as the time between pulse peaks.

## RESULTS

### A Simplified PKA Model

We begin by studying the behavior of a simplified model of the protein kinase A (PKA) system. The regulation of PKA involves multiple steps and has been modeled previously as limit cycle oscillations with deterministic (Garmendia-Torres et al., 2007; Gonzales et al., 2013) and stochastic (Besozzi et al., 2012; Gonze et al., 2008) approaches in a very detailed manner. Here, we propose a much simpler model for PKA regulation based on a single negative feedback, which is shown schematically in Figure 1A. The active form of PKA is given by its catalytic subunit $C$, which is generated when cyclic adenosine monophosphate (cAMP), denoted by $A$, causes its dissociation from the inhibitory regulatory subunit $R$. $C$ activates the phosphodiesterase (Hu et al., 2010; Ma et al., 1999), represented by $P_a$, which in turn promotes the degradation of $A$, thereby allowing $C$ and $R$ to re-associate into the inactive complex again, leading to a negative feedback of $C$ on itself. These processes are represented by the following system of coupled ordinary differential equations:

$$\frac{dC}{dt} = 2\left(\alpha A^2 (C_{tot} - C) - \beta R C^2\right) \qquad \text{(Equation 1)}$$

$$\frac{dR}{dt} = \alpha A^2 (C_{tot} - C) - \beta R C^2 + \Lambda - \delta R \quad \text{(Equation 2)}$$

$$\frac{dA}{dt} = k_s - \frac{k_d P_a A}{k_3 + A} \quad \text{(Equation 3)}$$

$$\frac{dP_a}{dt} = \frac{\gamma C (P_{tot} - P_a)}{k_1 + P_{tot} - P_a} - \frac{\varepsilon P_a}{k_2 + P_a}. \quad \text{(Equation 4)}$$

The model assumes that the total amounts of the catalytic subunit and phosphodiesterase are conserved ($C_{tot}$ and $P_{tot}$, respectively) as in Garmendia-Torres et al. (2007) and Gonze et al. (2008). In particular, $P_a$ follows a phosphorylation-dephosphorylation cycle in which the enzymatic reactions can saturate (Equation 4). We include in Equation 2 a synthesis term $\Lambda$ and a degradation term $\delta R$ since the stability of the regulatory subunit $R$ has been shown to be important for catalytic PKA activity (Budhwar et al., 2010). Notice that these production and degradation terms are phenomenological and could account for any change in the levels of available $R$ to bind $C$, due, for instance, to subcellular relocalization, which is another relevant regulatory mechanism (Tudisca et al., 2010). We should also note that in its inactive form, PKA is a tetramer formed by two catalytic subunits and two regulatory subunits. The regulatory subunit is generally considered to be found either as a dimer bound to cAMP or in the inactive holoenzyme formed by two regulatory and two catalytic subunits (Galello et al., 2014; Rinaldi et al., 2010). Therefore, for simplicity, we disregard monomeric regulatory subunits and consider only the dimeric form, which we represent by the variable $R$. We also consider the constant synthesis of $A$ and a saturating degradation following Garmendia-Torres et al. (2007) and Gonze et al. (2008). Moreover, instead of modeling explicitly the binding of cAMP to the regulatory subunit (Garmendia-Torres et al., 2007), we assume that $A$ favors the dissociation of $C$ in a nonlinear, concentration-dependent manner. In order to account for the fact that four molecules of cAMP bind the R homodimer, we assume a certain degree of cooperativity in its effect (not too large to avoid placing too much of a weight on this nonlinearity).

As a downstream target of $C$, we include Msn2 ($M$) phosphorylation and dephosphorylation, which we assume to reflect cytoplasmic ($M_c$) and nuclear ($M_n$) localizations, respectively, under constant overall concentration ($M_{tot}$):

$$\frac{dM_n}{dt} = \frac{a (M_{tot} - M_n)}{k_4 + M_{tot} - M_n} - \frac{b C M_n}{k_5 + M_n}. \quad \text{(Equation 5)}$$

Msn2 nuclear localization is inhibited by $C$. Therefore, we are interested in the capability of the model to exhibit downregulation pulses of $C$ in response to noise, as these would correspond to pulses of Msn2 nuclear localization. Since the number of molecules in the PKA system is large (Ghaemmaghami et al., 2003), we hypothesize that fluctuations are most likely to come from extrinsic sources that lead to variations in the reaction rates governing the system, rather than intrinsic noise due to a low number of molecules in the PKA system itself. In particular, given that the stability of the regulatory subunit has been shown to be relevant for PKA activity (Budhwar et al., 2010; Tudisca et al., 2010), we consider that its levels can fluctuate over time and study the response of the system to perturbations in its degradation rate ($\delta$).

For an appropriate parameter regime, a 2-fold increase in the degradation rate of $R$ during 15 s was enough to increase $C$ levels 10% over the steady state, leading to a subsequent inactivation pulse in $C$ with a reduction of more than 50% (Figure 1B). Such an inactivation pulse is generated as follows: the decrease in $R$ during the perturbation causes a small increase in $C$, which in turn significantly increases the levels of active phosphodiesterase $P_a$, causing a quick drop in the levels of $A$. This then causes a decrease in $C$ that results into a pulse of $C$ deactivation. When $C$ levels drop, $P_a$ returns to basal levels, and therefore $A$ increases again, eventually bringing all of the system back to the steady state and finishing the pulse. The inactivation pulse in $C$ causes a downstream activation of $M_n$ (Figure 1B, bottom). Notice that the perturbation point is not playing any role in the pulse beyond initially increasing $C$ levels, and thus any other fluctuation that would increase $C$ levels would result in the same behavior.

In order to explore the capability of the system to pulse in the presence of a dynamic noisy input, we introduced stochasticity into the rate of $R$ degradation. Since extrinsic fluctuations in the levels or activity of proteins are unlikely to be instantaneous, we assumed the noise to have a certain correlation time $\tau$, such that it can be modeled by an Ornstein-Uhlenbeck process:

$$\frac{dR}{dt} = \alpha A^2 (C_{tot} - C) - \beta R C^2 + \Lambda - e^{\eta} \delta R \quad \text{(Equation 6)}$$

$$\frac{d\eta}{dt} = -\frac{\eta}{\tau} + \frac{\sqrt{D}}{\tau} \xi(t), \quad \text{(Equation 7)}$$

where $\xi(t)$ is a Gaussian white noise of zero mean and intensity 1, and the exponential in the last term of Equation 6 is added so that the noise in the degradation of $R$ has a log-normal distribution (a common assumption for biomolecules; Rosenfeld et al., 2005).

We then performed simulations of this system using the stochastic-Heun algorithm (Toral and Colet, 2014) and observed that indeed the system exhibits pulses (Figure 1C). As shown in Figure 1D, small fluctuations are largely filtered out, but once $C$ increases over a certain threshold, a deactivation pulse follows, with larger increases being followed by larger decreases until the response saturates due to $A$ being fully degraded.

In order to confirm that the deactivations are indeed the result of the mechanism explained above and not just a mere reflection of the fluctuations in $R$, we computed the cross-correlation function between $e^{\eta}$ and C. We expect that high $\eta$ leads to increases in $R$ degradation and therefore an increase in free $C$ levels. This should lead to a positive correlation between the two variables at short lags, which corresponds to the positive peak at almost zero lag in Figure 1E. On the other hand, if the increase in $C$ triggers a pulse, this should lead to a decrease in $C$ sometime after, resulting in a negative peak in the cross-correlation function, which is also the case. In contrast, this negative peak is not observed if the feedback is disrupted by preventing the time evolution of $A$ and $P_a$ (Figure 1F), such that now the fluctuations in $C$ are just mirroring those in $R$.

Therefore, this system is capable of actively converting initially small increases in $C$ into large deactivation pulses with just a negative feedback loop. The duration of the pulses is around 2 min (Figure 1G), and since the pulses arise from noise and are not just noisy oscillations, the distribution of times between pulses has a long tail (Figure 1H), in agreement with the experimental data in Box Figure.

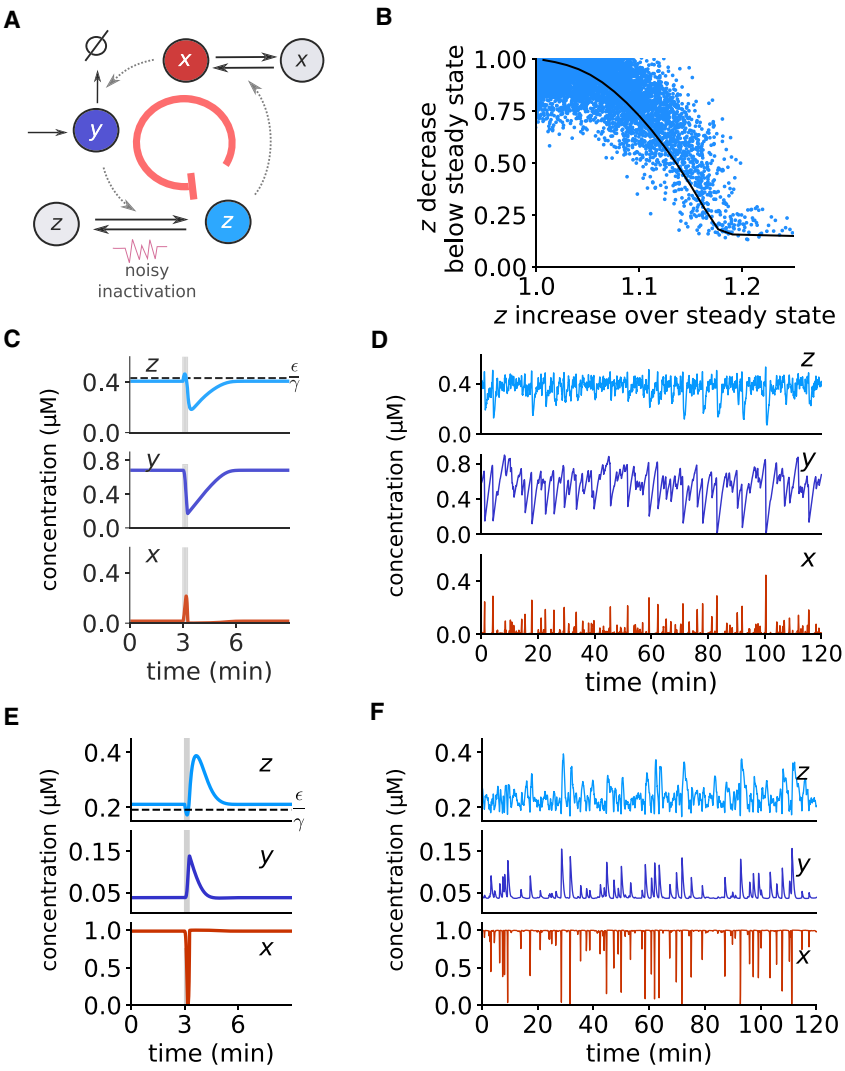


**Figure 2. Stochastic Pulses from a General 3-Variable Negative Feedback Loop**

(A) Scheme of the model.

(B–D) Inactivation pulses. (B) Input-output response of the system, calculated as in Figure 1D. (C) In response to a 30% reduction of $z$ deactivation rate $\beta$ during 15 s (gray shaded area), the system exhibits a pulse of $z$ inactivation. Parameter values: $k_s$ = 0.28 $\mu$Mmin$^{-1}$, $k_d$ = 17.85 min$^{-1}$, $k_3$ = 0.01 $\mu$M, $\alpha$ = 10 $\mu$M$^{-1}$min$^{-1}$ $\beta$ = 10 min$^{-1}$, $\gamma$ = 46.4 min$^{-1}$, $\varepsilon$ = 20 $\mu$M min$^{-1}$, $k_1$ = 0.0015 $\mu$M, $k_2$ = 0.001 $\mu$M, $z_{tot}$ =1 $\mu$M, and $x_{tot}$ = 1 $\mu$M. (D) Stochastic simulations with $D$=0.025 and $\tau$=15 s and same parameter values as in (C).

(E and F) Activation pulses. (E) Activation pulse in response to a 2-fold increase in $\beta$ during 15 s (gray shaded area). Parameter values: $k_s$ = 0.75 $\mu$Mmin$^{-1}$, $k_d$ = 0.964 min$^{-1}$, $k_3$ = 0.01 $\mu$M, $\alpha$ = 15 $\mu$M$^{-1}$min$^{-1}$, $\beta$ = 2.1 min$^{-1}$, $\gamma$ = 574.2 min$^{-1}$, $\varepsilon$ = 110 $\mu$Mmin$^{-1}$, $k_1$ = 0.0015 $\mu$M, $k_2$ = 0.001 $\mu$M, $z_{tot}$ = 1 $\mu$M, and $x_{tot}$ = 1 $\mu$M. (F) Stochastic simulations for the same parameters as in (E), with D = 0.05 and $\tau$=15 s.

See also Figures S1 and S2.

## A General Negative Feedback Model for Stochastic Pulsing

In order to simplify the previous model to a more general negative feedback motif, we next reduced the system to three variables by converting the $C$ activation process into an activation-deactivation cycle (Figure 2A) with its total concentration conserved and by assuming mass action kinetics. To emphasize the theoretical generality of such a model, we have relabeled the variables $P_a$, $A$, and $C_a$ into $x$, $y$, and $z$, respectively, leading to the following deterministic model:

$$\frac{dx}{dt} = \frac{\gamma\, z\, (x_{tot} - x)}{k_1 + x_{tot} - x} - \frac{\varepsilon\, x}{k_2 + x} \qquad \text{(Equation 8)}$$

$$\frac{dy}{dt} = k_s - \frac{k_d\, x\, y}{k_3 + y} \qquad \text{(Equation 9)}$$

$$\frac{dz}{dt} = \alpha\, y\, (z_{tot} - z) - \beta\, z. \qquad \text{(Equation 10)}$$

In this case, we perturbed (decreased) the $z$ deactivation rate $\beta$, and again this triggered a small increase in $z$ and a large decrease in response (Figure 2C). We also performed stochastic simulations, assuming a noisy $z$ deactivation rate, after modifying the corresponding equation accordingly:

$$\frac{dz}{dt} = \alpha\, y\, (z_{tot} - z) - e^{\eta}\, \beta\, z \qquad \text{(Equation 11)}$$

$$\frac{d\eta}{dt} = -\frac{\eta}{\tau} + \frac{\sqrt{D}}{\tau}\xi(t). \qquad \text{(Equation 12)}$$

Again, stochastic simulations of the model exhibited a nonlinear input-output response (Figure 2B) and inactivation pulses in $z$ (Figure 2D).

As explained in the previous section, we have used extrinsic noise in our simulations because the number of molecules in the PKA system is large. However, in many cellular systems, the total amount of molecules of the system components is low, such that noise arises from the stochasticity in the molecular reactions. In order to test whether such intrinsic noise is also able to generate $z$ downregulation pulses in this generalized circuit architecture, we performed stochastic simulations of this model

using the Gillespie algorithm and found that pulses also appeared in this case (Figures S1A and S1B).

This simplified model provides insight into the key features underlying the inactivation pulses in the target variable $z$ ($C$ in the PKA model in Figure 1). First, the dynamics of $x$ (corresponding to the phosphodiesterase in the PKA model) are in a zero-order kinetics regime, since $k_1$ and $k_2$ are very small in relationship to the total concentration of $x$. In the biological system, this would correspond to a situation in which the enzymes responsible for these reactions are highly saturated, such that there is much more substrate than enzyme. Under these conditions, $x$ deactivation is essentially constant at rate $\varepsilon$, and the activation term becomes $\gamma z$, such that at steady state, $z$ determines $x$ levels in a switch-like manner, resulting in the well-studied phenomenon of zero-order ultrasensitivity (Goldbeter and Koshland, 1981). If $z$ is smaller than the threshold set by $\varepsilon/\gamma$ (dashed line in the top panel of Figure 2C), $x$ is inactive, whereas, when $z$ crosses the threshold, the steady state of $x$ abruptly switches to full activation. Since the steady-state levels of $z$ are very close to this threshold, small increases in $z$ due to noise are translated into relatively large increases in $x$ (shaded gray area in Figure 2C), as the variable moves toward the new steady state set by the higher $z$ values. However, the negative feedback starts acting: the degradation rate of $y$ increases, and if it responds faster than $z$, $y$ falls such that it leads to a subsequent decrease in $z$ below steady-state levels (downward pulse in the $z$ panel in Figure 2C). This then causes $x$ to return to basal (inactive) levels, with a subsequent increase in $y$ and $z$, and the pulse ends.

As in the case of the PKA model (Figure 1H), this general model also exhibits a long-tailed distribution of interpulse intervals (Figure S1C). A minimum noise intensity (parameter $D$ in Equation 12) is needed to reproduce the qualitative characteristics of the experimental observations: low noise strength leads to very sparse pulsing (cool-colored lines in Figure S1C), whereas pulses appear much more often for larger noise intensities (warm-colored lines in Figure S1C). This is consistent with the fact, as described above, that for a pulse to be generated, $z$ has to be perturbed sufficiently to allow $x$ to increase and, subsequently, $y$ and $z$ to decrease. The distributions of pulse durations (Figure S1D) and amplitudes (Figure S1E) are much less dependent on noise.

## A Pulsatile 2-Dimensional Model of a Negative Feedback

In order to gain further understanding of the system, we next simplified it to two variables, with a repressor ($x$) and an activator ($y$) (Figure 3A), such that the system can be studied in the phase plane. After removing species $z$, $x$ is now directly activated by $y$, which will be the considered target. In its nondimensional form, the model reads

$$\frac{dx}{dt} = \frac{\alpha_2\, y\, (1-x)}{h_2 + 1 - x} - \frac{x}{h_{d2} + x} \qquad \text{(Equation 13)}$$

$$\frac{dy}{dt} = \alpha_1 - \frac{\delta_1\, x\, y}{1+y}. \qquad \text{(Equation 14)}$$

In an appropriate parameter regime, the system responds to an increase in the activator $y$ with a subsequent large decrease (Figure 3B, blue line). When looking at the trajectory of the system in the phase plane (Figure 3C), we observe that the increase in $x$ caused by the increase in $y$ (gray line) forces the system to return to the steady state with an undershoot (black line) caused by the almost vertical downward flow early after the perturbation. Since the steady state is at the point where the nullcline corresponding to Equation 13 (orange) rapidly bends downward, the system is driven toward the steady state following the nullcline and without spiraling. On the other hand, if the two nullclines cross further to the right (in the plateau of the orange nullcline), damped oscillations occur instead (Figures 3D and 3E). It is well known that damped oscillations in a negative feedback system can become sustained for a sufficiently long delay (Novák and Tyson, 2008). Mathematically, such delay can be given by additional intermediate variables. Indeed, the three-variable model of the previous section can enter a sustained oscillatory regime through a supercritical Hopf bifurcation upon a single parameter change, which moves the system from steady to pulsatile to oscillatory dynamics (Figures S2A and S2B). This analysis shows that the pulsatile regime corresponds to a region in parameter space close to the bifurcation point where the steady state remains essentially constant. Upon most single-parameter variations around this point, the system still responds to a small perturbation with a well-defined pulse (Figure S2C).

## The Same Network Architecture Can Generate Activation and Deactivation Pulses

Notably, the $dx/dt$ (orange) nullcline in Figure 3C is symmetric, suggesting that a similar mirror behavior can occur if the steady state of the system is such that basal levels of the repressor ($x$) are high. Indeed, by increasing $\alpha_1$, the blue nullcline shifts; and after slightly adjusting the other rates, now the steady state moves to the other bending point, and the system exhibits $y$ activation pulses in response to a previous decrease in its levels (Figures 3F and 3G). In order to confirm the generality of this finding beyond two variables, we went back to the 3-variable model shown in Figure 2 and found that it also exhibits activation pulses after readjusting the parameters such that, at steady state, $x$ is high and $y$ and $z$ are lower (Figures 2E and 2F).

The phase-plane analysis of the 2-dimensional system also clarifies the role of zero-order ultrasensitivity, as discussed for the 3-variable model. The capacity of the system to respond to a given perturbation requires the bending of the orange nullcline close to the steady state. Therefore, the inactivation pulses require saturation in the deactivation of $x$ (small $h_{d2}$, compare the two columns in Figure S3A for a configuration that allows pulses—left column—and one that does not—right column), while the activation pulses require saturation in the activation of $x$ (small $h_2$, compare the two rows in Figure S3B).

Finally, we found that the behavior is not sensitive to the mechanism of repression since the same results are obtained if the repressor inhibits activator production rather than increases its degradation (Figure S4).

## DISCUSSION

Negative feedbacks are well known to produce oscillations (Novák and Tyson, 2008) and in combination with positive

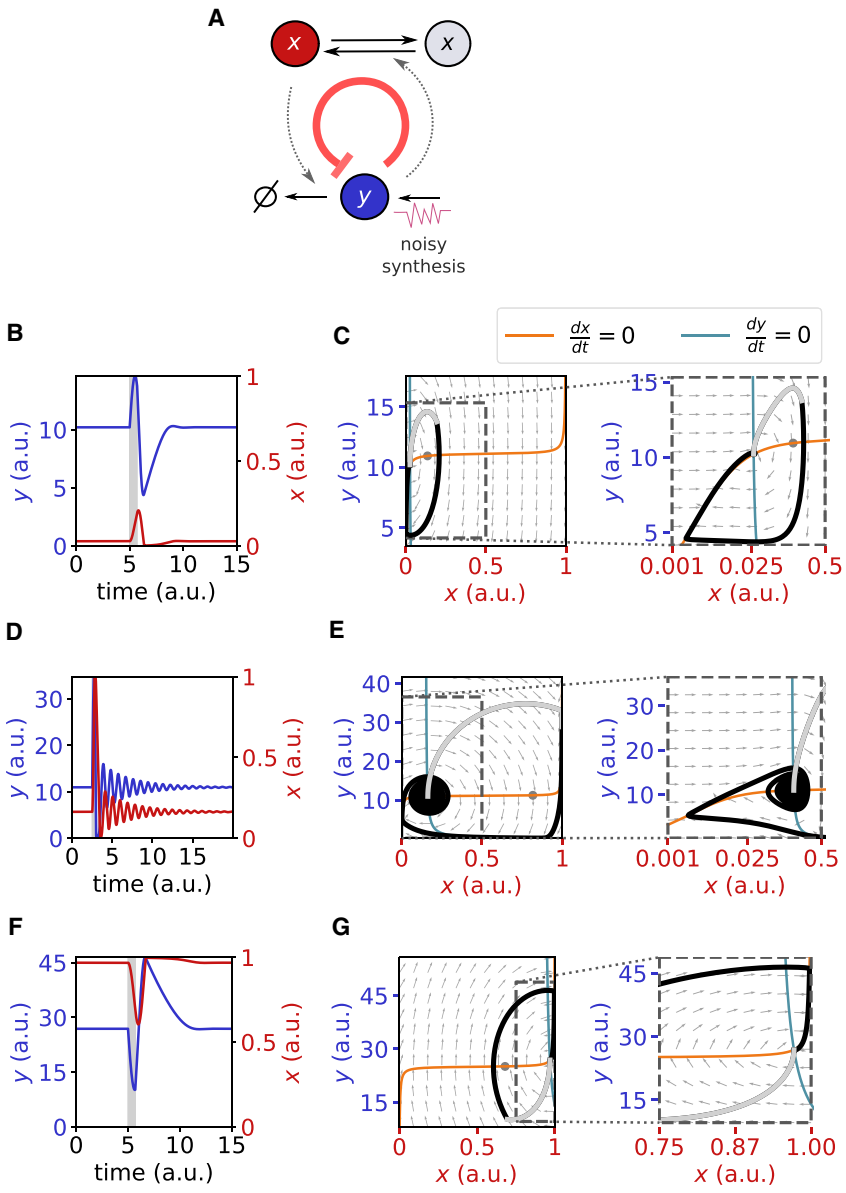


**Figure 3. Pulsing in a 2-Variable Activator-Repressor Model**

(A) Scheme of the model. The activator ($y$) activates the repressor ($x$), which degrades the former.

(B) Inactivation pulse in response to a 5-fold increase in $\alpha_1$ during 0.7 time units. Parameters (in arbitrary units): $\alpha_1$ = 3.5, $\delta_1$ = 140, $\alpha_2$ = 0.09, $h_2$ = 0.0025, and $h_{d2}$ = 0.0025. Shaded gray area indicates the time during which the system is perturbed.

(C) Nullclines and trajectory on the phase plane during the perturbation (gray line) and upon its release (black line), corresponding to the simulation in (B). Arrows indicate the direction of the flow; size has been normalized for clarity and does not reflect magnitude. The right panel is an inset of the region highlighted by a dashed square on the left panel, to better appreciate the region around the fixed point. Notice that here the $x$ axis is in log scale. The gray dot indicates the fixed point of the system corresponding to the perturbed state.

(D) Damped oscillations in response to a 5-fold increase in $\alpha_1$ during 0.7 time units. $\alpha_1$=25, rest of parameters as in (B).

(E) Nullclines and trajectory on the phase plane corresponding to the simulation in (D), as explained in panel (C).

(F) Upward pulse in response to a 30% decrease in $\alpha_1$ during 0.7 time units. Parameters (in arbitrary units): $\alpha_1$=140, $\delta_1$=150, $\alpha_2$=0.04, $h_2$=0.0025, $h_{d2}$=0.0025.

(G) Nullclines and trajectory on the phase plane, as in panel (C). Notice that here the x axis is no longer in log scale.

See also Figures S3 and S4.

feedback can also underlie the generation of noise-driven stochastic pulses (Locke et al., 2011; Rué and Garcia-Ojalvo, 2011). We have shown here that in fact, the positive feedback is not always required for the latter, and a negative feedback loop alone can generate pulses driven by noise under appropriate circuit architecture and timescales.

To study how a negative feedback can produce stochastic pulses, we started with a simplified model of the yeast PKA pathway, since pulses in Msn2 nuclear localization have been typically attributed to those in its upstream regulator PKA (Garmendia-Torres et al., 2007; Gonze et al., 2008; Hao and O'Shea, 2011). Our analysis shows that the PKA pathway could exhibit pulses of PKA inactivation that could lead to the dephosphorylation of Msn2 and a subsequent pulse of nuclear localization. This mechanism can explain the long-tail distribution of interpulse intervals that is observed experimentally, which is difficult to attain under a noisy oscillatory regime.

However, Msn2 is regulated by other kinases such as Snf1 and Hog1 and phosphatases such as PP1, which are important to fully explain the Msn2 response to stress identity and strength (Jiang et al., 2017; Petrenko et al., 2013). Even within the PKA system considered here, we have made a number of simplifications, such as ignoring the multiple phosphorylation sites on Msn2 (Hao et al., 2013), the differences between the phosphodiesterases PDE1 and PDE2, a second negative feedback on the production of cAMP (Garmendia-Torres et al., 2007; Gonzales et al., 2013; Stewart-Ornstein et al., 2017), and the subcellular localization and transport of the circuit components, which are likely to refine the behavior. It should be noted that, to our knowledge, there has been no experimental study of yeast PKA dynamics at the single-cell level that has not relied on Msn2 as a reporter (see for instance Garmendia-Torres et al., 2007; Stewart-Ornstein et al., 2017). Although a recent report has shown irregular activation pulses of PKA in a mammalian cell line, this was not followed up on, since the main aim of that study was to describe a PKA reporter (Zhang et al., 2018). Thus, it will be interesting to analyze specifically the activity of PKA and see whether, in fact, it is pulsatile. Given that PKA has a large number of targets and is

conserved across species, elucidating the dynamical behavior of this protein is of broad importance for cell biology.

More generally, our results show how a system can pulse by transiently amplifying a small perturbation into a significant change in activity in the opposite direction, due to a negative feedback. In our circuits, this behavior crucially depends on the zero-order ultrasensitivity in the response of the repressor to the fluctuating activator, such that a small variation in the activator causes a large variation in the repressor, which leads to a pulse in the activator due to the negative feedback. Besides zero-order ultrasensitivity, there are other mechanisms that under appropriate parameter regimes produce ultrasensitivity in the response to an input, in the sense that small changes in the input are translated into comparatively large changes in the output. These include, for instance, molecular titration by an inhibitor, substrate competition, and various multistep processes (Ferrell and Ha, 2014a). Therefore, a variety of circuits could be built with such mechanisms coupled to an overall negative feedback with the potential to generate pulses in response to fluctuations.

Another requirement for pulse generation in our models is that the system variables must have appropriate timescales. This is clear in the three-variable model in Figures 2A and 2C: it is not sufficient that $x$ increases during the perturbation but that $y$ needs to be quickly degraded and $z$ has to follow slightly more slowly. If $y$ is made to respond more slowly, it cannot decrease enough to generate the deactivation pulse in $z$. On the other hand, if $z$ responds too fast, it will decrease too soon, leading to the return of $x$ to the steady state before $y$ has decreased sufficiently to generate the deactivation pulse in $z$. The fast response of the repressor $x$ results from a post-translational modification cycle (e.g., phosphorylation-dephosphorylation) that operates in a zero-order regime. This fast behavior of $x$ leads initially to a fast response of $y$ since the deactivation of the latter is assumed to be enzymatic and thus to depend linearly on $x$. Once $x$ decays, the $y$ deactivation term becomes very small, leading to a very slow relaxation of $y$. The separation of timescales thus relies on a fast species ($x$) that deactivates enzymatically another species ($y$), which in turn feeds back onto the first via a third species $z$, whose dynamics are also determined by post-transcriptional events.

We also notice that in our simplified 2-variable models, the deviations from the steady-state levels required to initiate the pulse irrespective of its direction are quite large, which was not the case when there was an additional intermediate variable. This suggests that some delay in the system is required in order for the system to be able to amplify sufficiently small initial noise-driven fluctuations.

Negative feedback with ultrasensitivity is well known to generate oscillations (Ferrell and Ha, 2014b), and in fact, our three-variable model is also capable of oscillating, with single parameters having the capacity to change the dynamical regime from nonresponsive, to pulsatile, to oscillating. As the experimental methods to study dynamical behavior at the single-cell level improve, it will be interesting to elucidate whether cells display one dynamics or another or even whether they can transition between such regimes, as recently reported for p53 (Mönke et al., 2017), and the functional relevance of that behavior.

## STAR★METHODS

Detailed methods are provided in the online version of this paper and include the following:

- CONTACT FOR REAGENT AND RESOURCE SHARING
- METHOD DETAILS

### SUPPLEMENTAL INFORMATION

Supplemental Information includes four figures and can be found with this article online at https://doi.org/10.1016/j.cels.2018.08.012.

### ACKNOWLEDGMENTS

This work was supported by the Spanish Ministry of Economy and Competitiveness and FEDER (project FIS2015-66503-C3-1-P) and by the Generalitat de Catalunya (project 2017SGR1054). R.M.C. acknowledges financial support from La Caixa Foundation. J.G.O. acknowledges support from the ICREA Academia programme and from the "María de Maeztu" Programme for Units of Excellence in R&D (Spanish Ministry of Economy and Competitiveness, MDM-2014-0370). Y.L. acknowledges the support from the National Natural Science Foundation of China (Grant No. 31771425) and the Thousand Young Talents Program of China. M.B.E. is a Howard Hughes Medical Institute Investigator. This work was supported by the National Science Foundation grant #1547056.

### AUTHOR CONTRIBUTIONS

Conceptualization, R.M.C., M.B.E., and J.G.O.; Methodology, R.M.C. and J.G.O.; Investigation, R.M.C. and E.R.; Formal Analysis, R.M.C. and E.R.; Resources, Y.L. and M.B.E.; Data Curation, R.M.C. and Y.L.; Writing Original Draft, R.M.C. and J.G.O.; Writing Review & Editing, all authors; Supervision, Y.L., M.B.E., and J.G.O.; Funding Acquisition, J.G.O.

### DECLARATION OF INTERESTS

The authors declare no competing interests.

Received: April 27, 2018
Revised: July 27, 2018
Accepted: August 23, 2018
Published: October 10, 2018

### REFERENCES

Abel, J.H., Drawert, B., Hellander, A., and Petzold, L.R. (2016). GillesPy: a Python package for stochastic model building and simulation. IEEE Life Sci. Lett. *2*, 35–38.

Albeck, J.G., Mills, G.B., and Brugge, J.S. (2013). Frequency-modulated pulses of ERK activity transmit quantitative proliferation signals. Mol. Cell *49*, 249–261.

Aoki, K., Kumagai, Y., Sakurai, A., Komatsu, N., Fujita, Y., Shionyu, C., and Matsuda, M. (2013). Stochastic ERK activation induced by noise and cell-to-cell propagation regulates cell density-dependent proliferation. Mol. Cell *52*, 529–540.

Barrett, L., Orlova, M., Maziarz, M., and Kuchin, S. (2012). Protein kinase A contributes to the negative control of Snf1 protein kinase in Saccharomyces cerevisiae. Eukaryot. Cell *11*, 119–128.

Besozzi, D., Cazzaniga, P., Pescini, D., Mauri, G., Colombo, S., and Martegani, E. (2012). The role of feedback control mechanisms on the establishment of oscillatory regimes in the Ras/cAMP/PKA pathway in S. cerevisiae. EURASIP J. Bioinform. Syst. Biol. *2012*, 10.

Budhwar, R., Lu, A., and Hirsch, J.P. (2010). Nutrient control of yeast PKA activity involves opposing effects on phosphorylation of the Bcy1 regulatory subunit. Mol. Biol. Cell *21*, 3749–3758.

Cai, L., Dalal, C.K., and Elowitz, M.B. (2008). Frequency-modulated nuclear localization bursts coordinate gene regulation. Nature *455*, 485–490.

Clewley, R., Sherwood, W., LaMar, M., and Guckenheimer, J. (2007). Pydstool, a software environment for dynamical systems modeling. http://pydstool.sourceforge.net.

Dalal, C.K., Cai, L., Lin, Y., Rahbar, K., and Elowitz, M.B. (2014). Pulsatile dynamics in the yeast proteome. Curr. Biol. *24*, 2189–2194.

Ferrell, J.E., Jr., and Ha, S.H. (2014a). Ultrasensitivity part II: multisite phosphorylation, stoichiometric inhibitors, and positive feedback. Trends Biochem. Sci. *39*, 556–569.

Ferrell, J.E., Jr., and Ha, S.H. (2014b). Ultrasensitivity part III: cascades, bistable switches, and oscillators. Trends Biochem. Sci. *39*, 612–618.

Galello, F., Moreno, S., and Rossi, S. (2014). Interacting proteins of protein kinase A regulatory subunit in Saccharomyces cerevisiae. J. Proteomics *109*, 261–275.

Garmendia-Torres, C., Goldbeter, A., and Jacquet, M. (2007). Nucleocytoplasmic oscillations of the yeast transcription factor Msn2: evidence for periodic PKA activation. Curr. Biol. *17*, 1044–1049.

Geva-Zatorsky, N., Rosenfeld, N., Itzkovitz, S., Milo, R., Sigal, A., Dekel, E., Yarnitzky, T., Liron, Y., Polak, P., Lahav, G., et al. (2006). Oscillations and variability in the p53 system. Mol. Syst. Biol. *2*, 2006.0033.

Ghaemmaghami, S., Huh, W.K., Bower, K., Howson, R.W., Belle, A., Dephoure, N., O'Shea, E.K., and Weissman, J.S. (2003). Global analysis of protein expression in yeast. Nature *425*, 737–741.

Goldbeter, A., and Berridge, M.J. (1996). Biochemical Oscillations and Cellular Rhythms: the Molecular Bases of Periodic and Chaotic Behaviour (Cambridge University Press).

Goldbeter, A., and Koshland, D.E., Jr. (1981). An amplified sensitivity arising from covalent modification in biological systems. Proc. Natl. Acad. Sci. USA *78*, 6840–6844.

Gonzales, K., Kayıkçı, O., Schaeffer, D.G., and Magwene, P.M. (2013). Modeling mutant phenotypes and oscillatory dynamics in the Saccharomyces cerevisiae cAMP-PKA pathway. BMC Syst. Biol. *7*, 40.

Gonze, D., Jacquet, M., and Goldbeter, A. (2008). Stochastic modelling of nucleocytoplasmic oscillations of the transcription factor Msn2 in yeast. J. R. Soc. Interface *5*, S95–S109.

Görner, W., Durchschlag, E., Martinez-Pastor, M.T., Estruch, F., Ammerer, G., Hamilton, B., Ruis, H., and Schüller, C. (1998). Nuclear localization of the C2H2 zinc finger protein Msn2p is regulated by stress and protein kinase A activity. Genes Dev. *12*, 586–597.

Görner, W., Durchschlag, E., Wolf, J., Brown, E.L., Ammerer, G., Ruis, H., and Schüller, C. (2002). Acute glucose starvation activates the nuclear localization signal of a stress-specific yeast transcription factor. EMBO J. *21*, 135–144.

Guantes, R., and Poyatos, J.F. (2006). Dynamical principles of two-component genetic oscillators. PLoS Comput. Biol. *2*, e30.

Hao, N., Budnik, B.A., Gunawardena, J., and O'Shea, E.K. (2013). Tunable signal processing through modular control of transcription factor translocation. Science *339*, 460–464.

Hao, N., and O'Shea, E.K. (2011). Signal-dependent dynamics of transcription factor translocation controls gene expression. Nat. Struct. Mol. Biol. *19*, 31–39.

Hu, Y., Liu, E., Bai, X., and Zhang, A. (2010). The localization and concentration of the PDE2-encoded high-affinity cAMP phosphodiesterase is regulated by cAMP-dependent protein kinase A in the yeast Saccharomyces cerevisiae. FEMS Yeast Res. *10*, 177–187.

Jacquet, M., Renault, G., Lallet, S., De Mey, J., and Goldbeter, A. (2003). Oscillatory nucleocytoplasmic shuttling of the general stress response transcriptional activators Msn2 and Msn4 in Saccharomyces cerevisiae. J. Cell Biol. *161*, 497–505.

Jiang, Y., AkhavanAghdam, Z., Tsimring, L.S., and Hao, N. (2017). Coupled feedback loops control the stimulus-dependent dynamics of the yeast transcription factor Msn2. J. Biol. Chem. *292*, 12366–12372.

Levine, J.H., Lin, Y., and Elowitz, M.B. (2013). Functional roles of pulsing in genetic circuits. Science *342*, 1193–1200.

Lin, Y., Sohn, C.H., Dalal, C.K., Cai, L., and Elowitz, M.B. (2015). Combinatorial gene regulation by modulation of relative pulse timing. Nature *527*, 54–58.

Locke, J.C.W., Young, J.W., Fontes, M., Hernández Jiménez, M.J., and Elowitz, M.B. (2011). Stochastic pulse regulation in bacterial stress response. Science *334*, 366–369.

Loewer, A., Batchelor, E., Gaglia, G., and Lahav, G. (2010). Basal dynamics of p53 reveal transcriptionally attenuated pulses in cycling cells. Cell *142*, 89–100.

Ma, P., Wera, S., Van Dijck, P., and Thevelein, J.M. (1999). The PDE1-encoded low-affinity phosphodiesterase in the yeast Saccharomyces cerevisiae has a specific function in controlling agonist-induced cAMP signaling. Mol. Biol. Cell *10*, 91–104.

Mangan, S., Itzkovitz, S., Zaslaver, A., and Alon, U. (2006). The incoherent feed-forward loop accelerates the response-time of the gal system of Escherichia coli. J. Mol. Biol. *356*, 1073–1081.

Martinez-Corral, R., and Garcia-Ojalvo, J. (2017). Modeling cellular regulation by pulsatile inputs. Curr. Opin. Syst. Biol. *3*, 23–29.

Mönke, G., Cristiano, E., Finzel, A., Friedrich, D., Herzel, H., Falcke, M., and Loewer, A. (2017). Excitability in the p53 network mediates robust signaling with tunable activation thresholds in single cells. Sci. Rep. *7*, 46571.

Nicastro, R., Tripodi, F., Gaggini, M., Castoldi, A., Reghellin, V., Nonnis, S., Tedeschi, G., and Coccetti, P. (2015). Snf1 phosphorylates adenylate cyclase and negatively regulates protein kinase A-dependent transcription in Saccharomyces cerevisiae. J. Biol. Chem. *290*, 24715–24726.

Novák, B., and Tyson, J.J. (2008). Design principles of biochemical oscillators. Nat. Rev. Mol. Cell Biol. *9*, 981–991.

Petrenko, N., Chereji, R.V., McClean, M.N., Morozov, A.V., and Broach, J.R. (2013). Noise and interlocking signaling pathways promote distinct transcription factor dynamics in response to different stresses. Mol. Biol. Cell *24*, 2045–2057.

Purvis, J.E., and Lahav, G. (2013). Encoding and decoding cellular information through signaling dynamics. Cell *152*, 945–956.

Rinaldi, J., Wu, J., Yang, J., Ralston, C.Y., Sankaran, B., Moreno, S., and Taylor, S.S. (2010). Structure of yeast regulatory subunit: a glimpse into the evolution of PKA signaling. Structure *18*, 1471–1482.

Rosenfeld, N., Young, J.W., Alon, U., Swain, P.S., and Elowitz, M.B. (2005). Gene regulation at the single-cell level. Science *307*, 1962–1965.

Rué, P., and Garcia-Ojalvo, J. (2011). Gene circuit designs for noisy excitable dynamics. Math. Biosci. *231*, 90–97.

Sanft, K.R., Wu, S., Roh, M., Fu, J., Lim, R.K., and Petzold, L.R. (2011). StochKit2: software for discrete stochastic simulation of biochemical systems with events. Bioinformatics *27*, 2457–2458.

Schultz, D., Ben Jacob, E., Onuchic, J.N., and Wolynes, P.G. (2007). Molecular level stochastic model for competence cycles in Bacillus subtilis. Proc. Natl. Acad. Sci. USA *104*, 17582–17587.

Shankaran, H., Ippolito, D.L., Chrisler, W.B., Resat, H., Bollinger, N., Opresko, L.K., and Wiley, H.S. (2009). Rapid and sustained nuclear-cytoplasmic ERK oscillations induced by epidermal growth factor. Mol. Syst. Biol. *5*, 332.

Stewart-Ornstein, J., Chen, S., Bhatnagar, R., Weissman, J.S., and El-Samad, H. (2017). Model-guided optogenetic study of PKA signaling in budding yeast. Mol. Biol. Cell *28*, 221–227.

Süel, G.M., Garcia-Ojalvo, J., Liberman, L.M., and Elowitz, M.B. (2006). An excitable gene regulatory circuit induces transient cellular differentiation. Nature *440*, 545–550.

Sunnåker, M., Zamora-Sillero, E., Dechant, R., Ludwig, C., Busetto, A.G., Wagner, A., and Stelling, J. (2013). Automatic generation of predictive dynamic models reveals nuclear phosphorylation as the key Msn2 control mechanism. Sci. Signal. *6*, ra41.

Tomida, T., Takekawa, M., and Saito, H. (2015). Oscillation of p38 activity controls efficient pro-inflammatory gene expression. Nat. Commun. *6*, 8350.

Toral, R., and Colet, P. (2014). Stochastic Numerical Methods: An Introduction for Students and Scientists (Wiley-VCH Press).

Tsai, T.Y.-C., Choi, Y.S., Ma, W., Pomerening, J.R., Tang, C., and Ferrell, J.E., Jr. (2008). Robust, tunable biological oscillations from interlinked positive and negative feedback loops. Science *321*, 126–129.

Tudisca, V., Recouvreux, V., Moreno, S., Boy-Marcotte, E., Jacquet, M., and Portela, P. (2010). Differential localization to cytoplasm, nucleus or P-bodies of yeast PKA subunits under different growth conditions. Eur. J. Cell Biol. *89*, 339–348.

Voigt, C.A., Wolf, D.M., and Arkin, A.P. (2005). The Bacillus subtilis sin operon: an evolvable network motif. Genetics *169*, 1187–1202.

Zambrano, S., Bianchi, M.E., Agresti, A., and Molina, N. (2015). Interplay between stochasticity and negative feedback leads to pulsed dynamics and distinct gene activity patterns. Phys. Rev. E Stat. Nonlin. Soft Matter Phys. *92*, 022711.

Zambrano, S., de Toma, I., Piffer, A., Bianchi, M.E., and Agresti, A. (2016). NF-κB oscillations translate into functionally related patterns of gene expression. Elife *5*, e09100.

Zavala, E., and Marquez-Lago, T.T. (2014). Delays induce novel stochastic effects in negative feedback gene circuits. Biophys. J. *106*, 467–478.

Zhang, Q., Huang, H., Zhang, L., Wu, R., Chung, C.I., Zhang, S.Q., Torra, J., Schepis, A., Coughlin, S.R., Kornberg, T.B., et al. (2018). Visualizing dynamics of cell signaling in vivo with a phase separation-based kinase reporter. Mol. Cell *69*, 334–346.

## STAR★METHODS

### CONTACT FOR REAGENT AND RESOURCE SHARING

Further information and requests for resources and reagents should be directed to and will be fulfilled by the Lead Contact, Jordi Garcia-Ojalvo (jordi.g.ojalvo@upf.edu).

### METHOD DETAILS

Deterministic simulations were performed using the *odeint* function from the Python Scipy library. Stochastic Langevin simulations were performed using a custom implementation in C code of the stochastic Heun algorithm (Toral and Colet, 2014), and Gillespie simulations were executed in StochKit2 (Sanft et al., 2011) through the Python package GillesPy (Abel et al., 2016). Bifurcation diagrams were performed with the Python package PyDSTool (Clewley et al., 2007). Data analysis and plotting was done in Python.